ACS OMEGA

Article

Cite This: ACS Omega 2019, 4, 6324−6330

http://pubs.acs.org/journal/acsodf

Ultrasensitive and Rapid-Response Sensor for the Electrochemical Detection of Antibiotic Residues within Meat Samples

Hunter S. Stevenson, Shubrath S. Shetty, Noel J. Thomas, Vikram N. Dhamu, Ashlesha Bhide, and Shalini Prasad*

Department of Bioengineering, University of Texas at Dallas, 800 W. Campbell Rd., Richardson, Texas 75083, United States

ABSTRACT: Antimicrobial use in livestock has emerged as a pressing global issue because of the rise of antimicrobial-resistant bacteria. Regulatory authorities across the globe have taken steps to discourage the misuse of these antibiotics by banning or limiting the use of medically important antibiotics in food animals. However, to ensure that food animals are not being administered antibiotics inappropriately, there is a need for a reliable, raid-response biosensor that can detect the presence of these antibiotic residuals in meat products. We have developed an affinity-based electrochemical biosensor for the label-free detection of ceftiofur residues in meat samples. The sensor uses a self-assembled immunoassay to target the ceftiofur biomarker by employing electrochemical impedance spectroscopy to probe the interfacial capacitive changes as ceftiofur binds to the sensor surface. We have demonstrated a platform that can detect ceftiofur within 15 min of introducing the sample at concentrations down to 0.01 ng/mL in 1× phosphate-buffered saline and 10 ng/mL in 220 mg ground turkey meat samples.

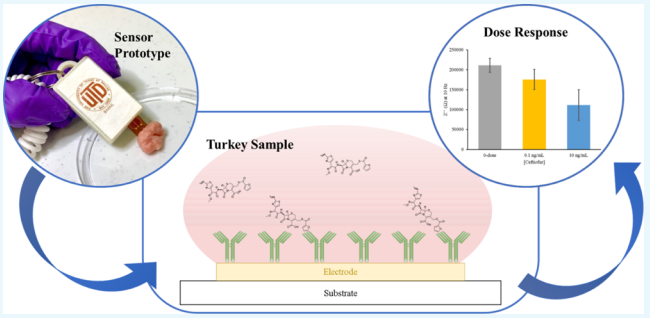

INTRODUCTION

Antimicrobials have played an essential role in the maintenance and care for livestock since the mid-twentieth century.[1,2] Today, antimicrobials are used in animal husbandry for a range of applications from therapeutic use to promoting feed efficiency. When administered at appropriate levels, these drugs exhibit bactericidal or antimicrobial effects by inhibiting the activity or growth of bacteria. However, when given in incorrect doses, bacterial drug resistance may arise through either selection through random genetic mutation or by horizontal plasmid exchange across an individual bacterium.[2,3] Evidence suggests that misusing antimicrobials has contributed to the rise of antimicrobial-resistant bacteria (ARBs).[4] Concern regarding the rise of ARBs has triggered an international response; the World Health Organization has made tackling ARBs a priority on their public health agenda and has released guidelines on the use of medically important antimicrobials in the food production industry.[2]

The repeated, widespread use of antimicrobial growth promoters (AGPs) in poultry, swine, and beef cattle has been linked to the rise in local antimicrobial-resistant bacterial populations.[3,5] General dosing in the animal's food leads to only partial metabolism of the antimicrobials and is passed into the manure.[1] The manure then harbors an environment for ARB proliferation and subsequent spread via run-off or percolation into rivers or water supplies.[2,3]

Growing demand for animal protein in the developing world has led to farming facilities to vertically integrate their livestock production—where many animals are raised in close proximity and in poor sanitary conditions.[6] Animals in these confined spaces are at high risk of catching and spreading illnesses, and so, antimicrobials are often used to curb the spread of disease. Multidrug-resistant ARBs have emerged in these developing countries, posing a potential worldwide risk to human health.[7,8] ARBs have been found not only in the treated animals, but also in their manure, local river water and crops, as well as the gut flora of farm employees and family members.[1,9]

Human health can be affected by antibiotics directly through residuals found in meat or indirectly through the selection of antibiotic-resistant strains of bacteria.[5,10] Gassner and Wuethrich (1994) demonstrated that residuals of chloramphenicol (a drug developed to treat typhoid) metabolites in meat products were linked to aplastic anemia in humans.[11] Perhaps more significantly, it was also believed that the overuse of chloramphenicol in animal feed may have led to drug resistance of the *Salmonella typhi*, the bacterium responsible for typhoid.[11]

Selection of resistant strains may occur in pathogens that can directly infect humans. Resistance may also be selected in bacteria that reside in animals which may be easily transmitted to humans (e.g., rabies, lymes disease, or salmonella). Consequences of infection from antibiotic-resistant bacteria range from prolonged illness to death depending on severity of the infection and treatment success rate.[12] Modern medicine

Received: December 17, 2018
Accepted: March 20, 2019
Published: April 4, 2019

DOI: 10.1021/acsomega.8b03534
ACS Omega 2019, 4, 6324−6330

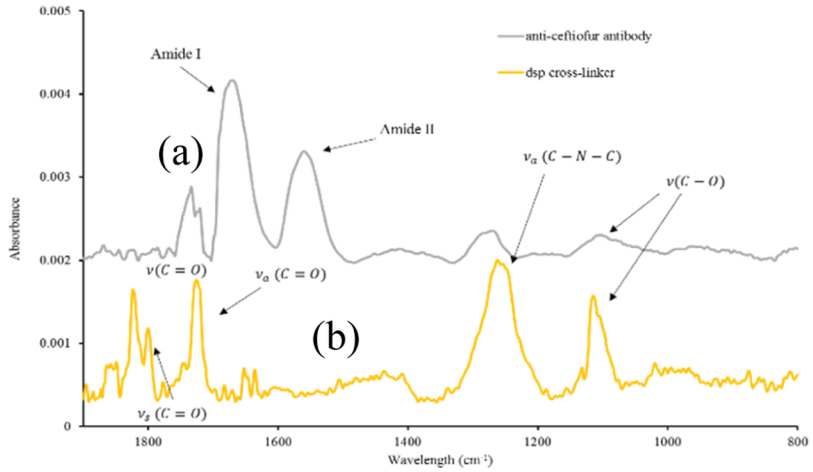

Figure 1. FTIR spectra validating the (a) DSP crosslinker immobilization onto bare Au surface and (b) bound anti-ceftiofur antibody conjugated to DSP crosslinker.

has provided numerous antibiotic variants, but some bacterial strains such as the multidrug-resistant *Staphylococcus aureus* (MDRSA) are not easily treatable by any antibiotic developed since the 1940s.[13]

These multidrug resistant bacteria have called for tighter regulations in the animal husbandry industry across the globe. The U.S. Food and Drug Administration, the European Union, and other regulatory bodies have taken strides to ensure the judicious use of medically important antimicrobial drugs in food-producing animals.[14] These efforts are defined as maximizing therapeutic efficiency and minimizing selection of resistant microorganisms. China, which produces over half of the world's pork, is among a short list of countries that places no restrictions on AGP use.[8,15] This high-volume use of antibiotics in these developing countries is believed to be one of the largest contributors to the increased environmental burden of antibiotic-resistant genes (ARGs)s.[8,15]

Among the many different classes of antibiotics, ceftiofur is a third-generation cephalosporin labeled for veterinary use.[12,15,16] Ceftiofur is often used to treat respiratory disease in swine, cattle, sheep, and goats as well as early mortality infections in chickens and turkeys.[17] Ceftriaxone—another third-generation cephalosporin—is critically important to human medicine as it is commonly used to treat bacterial infections in children. All cephalosporins share the same mechanism of action,[17] thus, resistance of bacteria toward these antibiotics is a major concern among medical and veterinary experts.[14] Studies have supported the notion that the use of ceftiofur in animal food products is a potential source of ceftriaxone-resistant salmonella infections in humans.[16,18,19]

As more countries are pressured to adopt regulations limiting the use of antibiotics, the regulatory burden has grown when ensuring the judicious use of antibiotics. A low-cost, reliable, and easy-to-use biosensor that can detect antibiotics in animal food products would not only reduce this regulatory burden but could also appeal to consumers who wish to verify that their food is antibiotic-free.

The current state-of-the-art antibiotic detection is achieved through the principle of microbial inhibition. The Charm KIS test, for example, utilizes bacteria in agar with a pH-indicator media.[20] When activated, the bacteria generate acid and the pH indicator changes colors. In the presence of an antibiotic, the bacterial growth is inhibited, and the test does not change colors. Although relatively easy to use, these tests are time consuming and do not provide quantitative results for regulatory enforcement purposes. Enzyme-linked immunosorbent assay (ELISA) and high-performance liquid chromatography (HPLC) have shown promise as potential analytical methods for identifying antibiotic residues in food. These tools have demonstrated isolation and identification of various antibiotics in animal tissue samples. However, large-scale and low-cost implementation of these systems remains a problem to be solved. ELISA often demonstrates good sensitivity and specificity, but it requires a relatively large volume of sample and must be run on a benchtop plate-reader by a trained scientist to interpret the results. HPLC analysis is relatively quick to perform, but uses large quantities of expensive organics and is difficult to implement on a handheld device.

Although some screening methods for detecting antibiotic residues exist,[21] these tests are either based on microbial growth inhibition rather than detection of the analyte itself or chromatographic methods, which are expensive and time-consuming. Efforts to incorporate nanomaterials in antibiotic biosensors have been emerging in the literature,[22] however, many of these biosensors either require labeling of the targeted antibiotic or have not demonstrated the ability to detect antibiotics in meat samples. Here, we have developed a novel affinity-based electrochemical biosensor that can rapidly detect ceftiofur residues directly in meat samples without the need for labeling of the target antibiotic.

Affinity-based immunosensors offer an attractive solution for scientists within the animal husbandry industry, as well as regulatory bodies and consumers for the detection of antibiotics in animal meat products. Affinity-based immunosensors leverage biomarker detection through a recognition element that specifically targets the biomarker of interest. The chemical reaction between the target biomarker and the recognition element is then transduced to a measure signal output related to the concentration of the targeted biomarker. Immunosensors, particularly electrochemical immunosensors, are an attractive solution for single-use biosensing because of their high sensitivity, selectivity, and scalable manufacturability.[23,24]

We have previously demonstrated many affinity-based biosensors using nonfaradaic electrochemical impedance

DOI: 10.1021/acsomega.8b03534
ACS Omega 2019, 4, 6324−6330

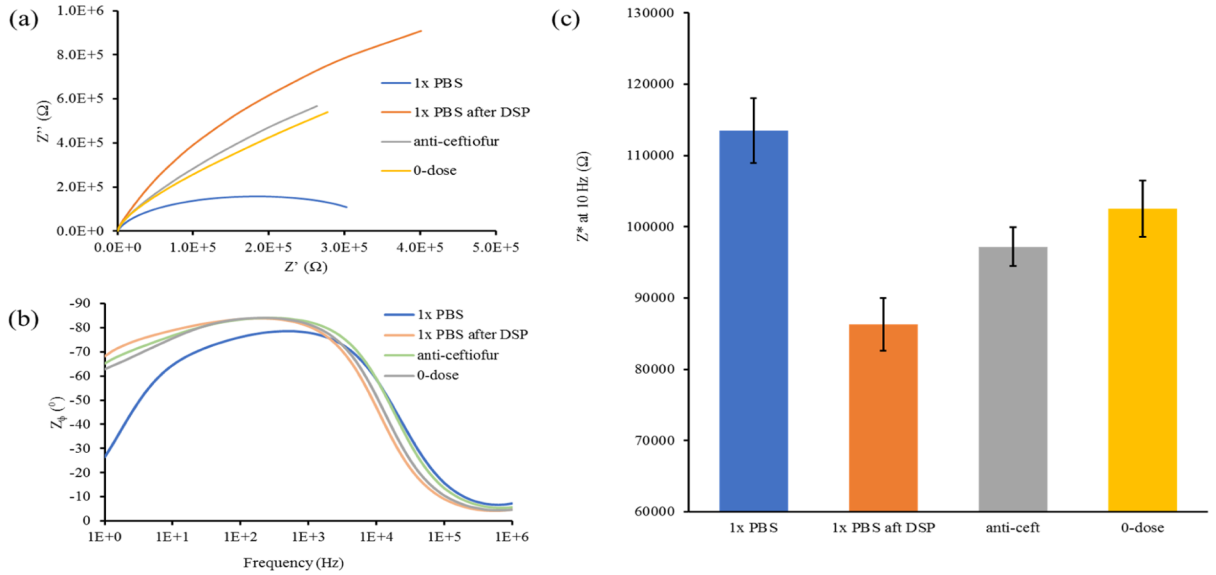

Figure 2. (a) Nyquist impedance plot, (b) Bode phase plot, and (c) extracted Z^* values at 10 Hz for EIS measurements to validate the chemisorption of the DSP crosslinker and subsequent anti-ceftiofur antibody.

spectroscopy (EIS) to detect a range of biomarkers for various agricultural and human health and wellness applications.[23,24] Here, we present an affinity-based biosensor that utilizes nonfaradaic EIS to detect the presence of antibiotics in turkey meat samples. A highly specific immunoassay is constructed on the sensor surface to encode specificity toward ceftiofur—the antibiotic of interest.

RESULTS AND DISCUSSION

Fourier-Transform Infrared Spectroscopy Surface Characterization. Chemisorption of the dithiobis-(succinimidyl propionate) (DSP) crosslinker and anti-ceftiofur antibody on the gold electrode surface was validated using Fourier-transform infrared spectroscopy (FTIR). Gold thin films were deposited on polyethylene terephthalate (PET) substrates using e-beam vapor deposition at parameters mimicking those used for sensor fabrication and FTIR analysis. Functionalization of the electrode surface was carried out as described in the previous section. Before FTIR measurements, each sample was rinsed thoroughly with distilled (DI) water, and then dried with N_2 air to rid the surface of any unbound material that may interfere with the analysis. The infrared spectra of surface-modified samples were recorded with a Nicolet iS50 FTIR spectrometer.

Absorbance spectral measurements were obtained with a scan resolution of 4 cm^{-1} for 64 scans in the spectral range of 4000−600 cm^{-1}. Absorption spectra were recorded for PET−gold surface conjugated to DSP molecules, and the gold surface with anti-ceftiofur antibodies linked via the DSP linker molecules. The absorbance peaks observed in the DSP spectrum of Figure 1 at 1799 and 1724 cm^{-1} indicate the symmetric and asymmetric carbonyl stretches, respectively, of the *N*-hydroxysuccinimide (NHS) ester. Furthermore, the peak at 1251 cm^{-1} confirms the presence of the asymmetric C−N−C stretch of the NHS ester, whereas the peak at 1112 cm^{-1} can be identified as the succinimide N−C−O stretch. Finally, the peak at 1822 cm^{-1} indicates the ester carbonyl stretch. The presence of these peaks is characteristic of a self-assembled monolayer (SAM) of DSP, confirming the chemisorption of DSP to the gold surface.

The reaction between the NHS group with the antibody's primary amine group can be noted in the anti-ceftiofur spectrum. The C−O bonds of the NHS ester are broken and react with primary amines of the antibody, resulting in a stable amide bond. Suppression of peaks associated with the NHS ester (1799, 1724, and 1251 cm^{-1}) is observed, whereas peaks at ∼1644 and ∼1552 cm^{-1} are indicative of amide I and amide II peaks. These results show a stable formation of the immunoassay through the binding of the anti-ceftiofur antibodies to the DSP-functionalized surface.

Electrochemical Impedance Spectroscopy. The electrochemical response was evaluated at each step of the immunoassay through EIS measurements. The bulk and interfacial phenomena were visualized using Nyquist impedance plots (Figure 2a), and values of the impedance modulus (Z^*) were extracted at 10 Hz to highlight the impedance changes as the immunoassay was chemisorbed onto the sensor surface as seen in Figure 2b.

A 1× phosphate-buffered saline (PBS) measurement was performed before any surface modifications to evaluate the baseline electrical double layer (EDL) properties at the electrode−electrolyte interface. In the absence of any surface modifications, the 1× PBS measurement exhibits a compressed semicircle in the Nyquist impedance plot, indicating a resistance-dominated system where hydrolysis and/or gold oxidation is occurring as charges leak across the electrode−electrolyte interface because of the applied dc bias. After subsequent binding of the DSP linker, a second 1× PBS measurement was taken to examine how the DSP monolayer impacts interfacial properties. When the DSP linker self-assembles, an insulative layer forms at the interface, both reducing the propensity for charge transfer across this interface and increasing the charge separation between the solvent ions and the electrode surface.

When extracting the impedance at 10 Hz (Figure 2c), the Z^* drops from 113 528 to 86 295 Ω after binding DSP to the gold electrode surface. The impedance drop is driven by changes in both the real and imaginary impedance response. The decrease in charge transfer across the interface is observed as a large reduction in the real impedance (Z'), a small increase in

DOI: 10.1021/acsomega.8b03534
ACS Omega 2019, 4, 6324−6330

imaginary impedance (Z''), and an increase in the semi-circle diameter of Figure 2a. Binding of the DSP molecules also creates a separation of charges and leads to a reduction in the EDL capacitance (hence, the increase in Z''), shifting the low frequency phase response toward −90° as seen in the Bode phase diagram in Figure 2b.

After DSP modified the surface, the addition of the antibody introduces excess charges at the electrode interface, resulting in a small increase in Z' as well as the phase. This increase is reflected in the overall impedance as the Z^* value at the antibody step was 97 208 Ω. A third 1× PBS measurement (0-dose) was taken to validate that the antibodies remain bound to the electrode surface. Although there was a slight increase in the Z^* value (to 102 537 Ω), there was no significant change observed between the antibody and the subsequent PBS, indicating that the NHS esters on the DSP molecule have reacted with the primary amines on the anti-ceftiofur antibody, anchoring them to the electrode surface.

Calibrated Dose Response in 1× PBS. The third 1× PBS measurement after the antibody also serves as a "blank" for subsequent ceftiofur dose steps. Doses of ceftiofur were prepared in 1× PBS from 0.1 to 10 ng/mL, and the resulting Nyquist capacitance plots are shown in Figure 3.

The measured concentration range was selected as it spans the typical concentrations measured in commercially available ceftiofur ELISA kits. As ceftiofur molecules bind to the immunoassay, the dielectric permittivity of the EDL is modulated.

Changes in impedance spectra because of biomarker binding are not always resolvable depending on the nature of the support matrix and the biomarker of interest. To address the poor resolution between ceftiofur concentrations, the impedance data is transformed into a complex capacitance, which highlights the storage characteristics occurring at the interface rather than resistive terms which are emphasized in EIS. A complex capacitance plot is shown in Figure 3a with the imaginary capacitance (C'') on the y-axis and the real capacitance (C') on the x-axis. Here, a semicircle is observed for every dose of ceftiofur with a diameter of ∼7.5 × 10^{-6} S, corresponding to the primary relaxation constant of the immunoassay.

A second, concentration-dependent semicircle manifests at lower frequencies with higher doses of the ceftiofur biomarker. This second semicircle appears due to a second relaxation process in response to the applied potential. The polar structure of the ceftiofur molecule likely introduces additional degrees of freedom when binding to the adsorbed immunoassay. However, further investigation into the immunoassay structure would need to be carried out before validating this claim. The percent change in impedance at 10 Hz was the calculated change for each concentration of ceftiofur with respect to the antibody measurement and plotted versus ceftiofur concentration between 0.01 and 100 ng/mL with the initial "0-dose" corresponding to a measurement in 1× PBS without any ceftiofur antigens.

When the ceftiofur molecule binds to the immunoassay, a second dipolar relaxation process emerges, raising the capacitance, and thus, decreasing the impedance response. For ceftiofur spiked in PBS, the impedance response varies with a dynamic range between 75967 Ω (0.01 ng/mL) and 67020 Ω (100 ng/mL), corresponding to a 26% to a 34% change with respect to a blank solution. A signal-to-noise ratio

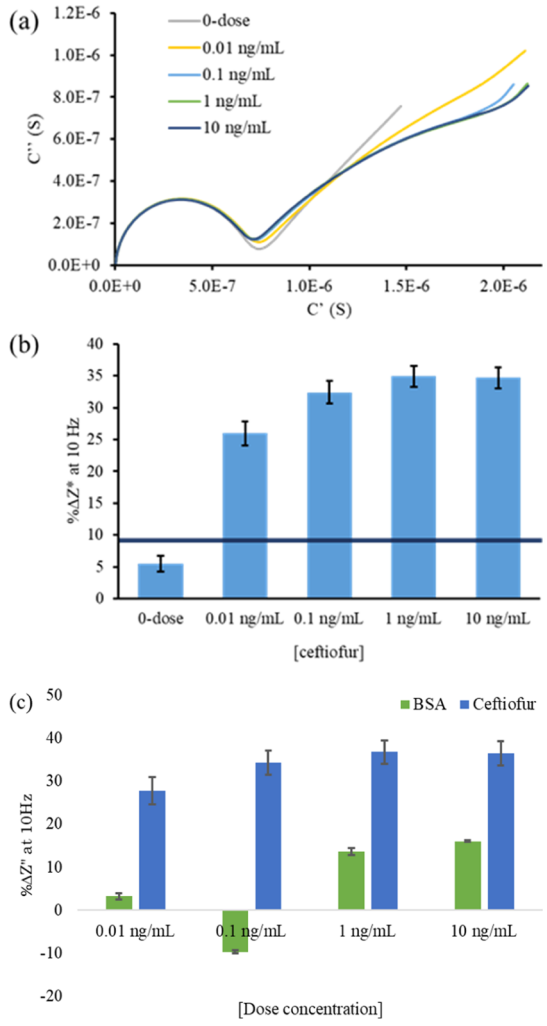

Figure 3. Calibrated dose response across varying concentrations of ceftiofur administered onto the sensor represented as (a) Nyquist capacitance plot, (b) percent change in impedance with respect to the antibody measurement at 10 Hz with SST in dark blue (n = 4), and (c) percentage change in impedance comparison with respect to the blank dose (1× PBS) at 10 Hz for nonspecific BSA (green) and specific ceftiofur (blue) for n = 3.

of 3 was selected to calculate the specific signal threshold (SST) impedance as indicated in the following equation

$$\mathrm{SST} = \mu_{\mathrm{blank}} + 3 \times \mathrm{SD}_{\mathrm{blank}} \quad (1)$$

The limit of detection (LOD) is identified as the lowest concentration of ceftiofur, which can be reliably and feasibly detected from a "blank" solution.

The LOD can be calculated by using the mean and standard deviation for the 1× PBS measurement after binding the antibody

$$\mathrm{LOD} = [\mathrm{ceftiofur}]_{\mathrm{low}} \text{ when } (\mu_{[\mathrm{ceftiofur}]} - \mathrm{SEM}_{[\mathrm{ceftiofur}]}) > \mathrm{SST} \quad (2)$$

The LOD was found by subtracting the SEM for each concentration of the ceftiofur ($\mathrm{SEM}_{[\mathrm{ceftiofur}]}$) from the mean $\mu_{[\mathrm{ceftiofur}]}$. This value was then compared to the SST for each concentration of ceftiofur, and the lowest concentration that exhibited a value larger than the SST was determined as the LOD. Concentrations at and above the LOD show significant

DOI: 10.1021/acsomega.8b03534
ACS Omega 2019, 4, 6324−6330

impedance responses indicating that ceftiofur is reliably detectable. Using eq 2, the LOD for ceftiofur was 0.01 ng/mL in 1× PBS. Although a lower LOD likely exists for ceftiofur in 1× PBS, as seen in Figure 3b, the 1× PBS dose response is meant to validate that varying doses will elicit a different electrochemical response, not to characterize the entire dynamic range of the sensor. Thus, 0.01 ng/mL was chosen as an acceptable lower LOD.

The ability of the biosensor to respond to ceftiofur in the presence of nonspecifics is defined as the specificity of the sensor. Robust biosensing requires evaluation of the non-specific responses obtained on interaction with the ceftiofur antibody with non-specific antibiotics and proteins. The specificity of the sensor is determined by using BSA (bovine serum albumin) as the nonspecific protein. The binding interaction between the anti-ceftiofur immobilized on the sensing platform and increasing dose concentrations of BSA is shown as a calibration dose response in Figure 3c. The percentage change in imaginary impedance with respect to the blank dose (1× PBS) is calculated at 10 Hz. The percentage change in imaginary impedance for the nonspecific protein, BSA, shows no dose-dependent response for increasing concentrations of BSA and is observed to be between 3.7 and 15% for BSA concentrations 0.01−10 ng/mL. However, the interaction between ceftiofur with its specific antibody shows an increasing dose response with increasing ceftiofur concentrations. The percentage change in imaginary impedance for increasing ceftiofur concentrations, 0.01−10 ng/mL, is observed to be 27−37%. The outcome of the specificity study is that nonspecific proteins, such as BSA, show minimum crossresponse to the immobilized ceftiofur antibody.

Calibrated Dose Response in Meat. Translating from 1× PBS to the turkey meat enhanced the resolution of bulk capacitive response as indicated by the Nyquist impedance plots shown in Figure 4a. This is likely because the turkey samples exhibited a more resistive response, implying a lower effective ionic content, thus enhancing the effect of interfacial bulk capacitance. To remove the effects from bulk solution resistance and focus on affinity binding at the interface, the imaginary impedance (Z'') was isolated and analyzed at the low-frequency spectrum to determine dose-dependent changes, as seen in Figure 4b.

The turkey samples act as a porous solid retaining the electrolyte within the meat. The addition of these porous boundaries interferes with the distance for the ions to travel in the bulk of the solution and is seen as an increase in the high frequency solution resistance. The low-frequency response of the sample is less impacted by the meat sample, as it measures interfacial properties and does not probe into the bulk of the solution. At the low frequency range, it is evident that as larger concentrations of ceftiofur are added to the meat samples, a decrease in Z'' is observed. This decrease is caused again by the binding of electrically charged ceftiofur molecules modulating the dielectric permittivity within the EDL. The LOD was again found for the ceftiofur doses in turkey meat. Here, SST was found using eq 3.

$$\mathrm{SST} = \mu_{\mathrm{blank}} + 2 \times \mathrm{SD}_{\mathrm{blank}} \quad (3)$$

The SST was 159 050.3 Ω. The LOD was then calculated using eq 2 for the doses in turkey meat, making the 10 ng/mL dose the only sample reliably distinguishable from the antibiotic-free meat. It can be concluded that the sensor performance is effective at detecting ultra-low concentrations of ceftiofur within meat samples, and the flexible sensor prototype would greatly reduce the time and financial burden to test meat samples for the presence of antibiotic residues.

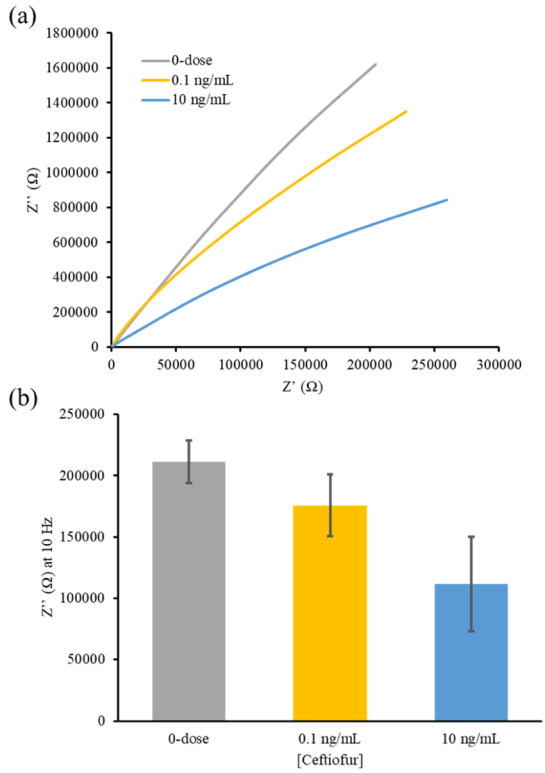

Figure 4. Calibrated dose response across varying concentrations of ceftiofur absorbed in turkey meat samples administered directly onto the sensor and represented as (a) Nyquist impedance plot and (b) Z''at 10 Hz (n = 3).

CONCLUSIONS

Antibiotic detecting in meat samples has tremendous importance in the livestock and consumer marketplace. As new strains of antibiotic-resistant bacteria continue to emerge, regulatory authorities, such as the FDA and USDA, will continue to place more restrictions on the use of medically important antibiotics in food animals. These restrictions place a larger financial and time burden on livestock farmers to comply with appropriate dosing of antibiotics and regulators to ensure compliance. To prevent these operations from being too costly or time consuming, a faster, cheaper method of antibiotic detection is needed.

This work proposes a low-cost, proof-of-concept biosensor for the detection of antibiotic residuals. Based on our review of literature in the public domain, this is the first impedimetric biosensor for the detection of antibiotics in meat samples. The biosensor demonstrates high sensitivity (LOD = 0.01 ng/mL) in a physiological buffer, without the use of any external labels or redox reagents. Monitoring both changes in EDL capacitance (through Nyquist impedance plots) and SAM dielectric capacitance (through Nyquist capacitance plots) allows for the detection medium to be readily swapped for other more complex samples, such as turkey meat. In the turkey meat samples, the sensor demonstrates a decreasing trend in the Z'' response at 10 Hz at concentrations of ceftiofur well below the current standard detection thresholds. Additionally, the sensor was still able to capture dose-dependent

DOI: 10.1021/acsomega.8b03534
ACS Omega 2019, 4, 6324−6330

changes within the meat samples with good sensitivity (LOD = 10 ng/mL). The higher limit of detection was due to the complex nature of the meat sample matrix. The porous nature of the meat interferes with the nonfaradaic current conduction, and physical contact of the meat sample onto the sensor surface may also impede access to the self-assembled immunoassay. However, this is—to our knowledge—the first demonstration of a label-free, electrochemical biosensor for the detection of any antibiotic material.

This work demonstrates strong feasibility toward a rapid, versatile antibiotic biosensor by characterizing the effect of a meat matrix on the immunosensor. An easy to use biosensor that can detect the presence antibiotic material directly in the meat samples would allow regulatory authorities, livestock farmers, and everyday consumers to better monitor the quality of their meat. Further refinement of the sensor architecture should be explored to validate antibiotic detection in contaminated meats, by exploring methods to first increase sensitivity on spiked meat matrices. Additionally, as antibodies can be produced for nearly any target antigen, it is feasible that this platform can be modulated to detect other antibiotics by replacing the anti-ceftiofur antibody within the immunoassay. Additionally, the sensor could be tested across a variety of meat samples. To increase the resolution for detection within meat samples, other surface modifications may be necessary to create a physical barrier between the meat sample and the immunoassay constructed on the sensor surface (e.g., hydrogel deposition or another physical polymer barrier). The barrier would prevent physical interaction between the meat sample and the immunoassay, likely leading to better stability and sensitivity. However, this work has demonstrated reproducible detection of antibiotic residues within meat samples, making this sensor platform as the first demonstration of in-meat electrochemical antibiotic biosensing.

EXPERIMENTAL SECTION

Sensor Fabrication Process. The biosensor was fabricated on PET substrates using the e-beam deposition technique. Electrodes were deposited using electron beam physical vapor deposition at a pressure of 5×10^{-6} Torr. The electrode patterns were deposited with 125 nm Au onto the precleaned PET substrate. A polydimethyl siloxane confinement well was prepared to restrict the sample fluid in a controlled volume around the site of the three electrodes. To prepare the sensors for electrochemical measurements, the surface of the gold electrodes and the PET substrate were rinsed with 70% isopropyl alcohol, and DI water to remove organic residues. The electrodes were then dried with inert N_2 gas to prepare the surface for self-assembly of the immunoassay. Construction of the immunoassay first chemisorbs a linker molecule to the electrode surface, and then binds a capture antibody for subsequent detection of a dynamic range of the ceftiofur antigen.

The linker molecule specific to our biosensor is the amine-reactive crosslinker DSP. DSP has a NHS ester that is highly reactive with the primary amines which are abundant in antibodies and a cleavable disulfide bond in the molecule's spacer arm that interacts with the electrode surface via gold–thiol interaction. DSP forms highly ordered SAMs,[25,26] which immobilize the anti-ceftiofur (α-ceftiofur) capture antibody. A 150 μL sample of 10 mM DSP was incubated on the bare sensor surface for 60 min. After DSP immobilization, a sample of 150 μL of 10 μg/mL α-ceftiofur antibody were incubated on the sensor surface for 90 min to ensure reaction with the DSP molecules. High-affinity of the ceftiofur antigen toward the α-ceftiofur antibody allows for rapid binding interactions. Specificity studies involved the interaction of increasing dose concentrations of 0.01–10 ng/mL BSA prepared in 1× PBS with the α-ceftiofur antibody.

Turkey Meat Matrix Preparation. Turkey meat samples were prepared from USDA-verified antibiotic free source to ensure that no ceftiofur residuals would be already present in the samples. The meat samples (220 mg) were first submerged in 300 μL of 1× PBS (control), a 0.1 ng/mL ceftiofur dose, or a 10 ng/mL ceftiofur dose for 15 min to ensure uptake of the ceftiofur antigen. The samples were then placed on the sensor and tested for affinity binding of the ceftiofur biomarker to the immunoassay. Further refinement of the incubation time may be necessary to ensure that the ceftiofur molecules are absorbed within the meat, however, we have demonstrated through our electrochemical measurements that the ceftiofur molecule was present in the meat sample upon testing.

Electrochemical Evaluation. Electrochemical experiments were performed using a Gamry Reference 600 potentiostat. Nonfaradaic EIS was used as a label-free approach to quantify impedance changes in the electric double-layer capacitance. An input 10 mV sinusoidal voltage with a dc bias of −0.3 V versus ref was applied at the working electrode, and then scanned across a frequency range of 1 Hz to 1 MHz (input parameters optimized previously).[27] The resultant current response was measured, and the complex impedance was calculated as the ratio of the input voltage to the output current. Ceftiofur doses were diluted in 1× Dulbecco's PBS (1× PBS) to obtain concentrations of 0.01–10 ng/mL for either sample. A "blank" sample (absent of the ceftiofur antigen) was tested after functionalization with the antibody to serve as a baseline measurement before administering subsequent doses.

After validating the electrochemical response to ceftiofur in a relatively low noise physiological buffer, the biosensor was then tested using turkey meat samples to characterize the feasibility as an antibiotic sensor for animal food products.

AUTHOR INFORMATION

Corresponding Author

*E-mail: Shalini.Prasad@utdallas.edu. Phone: 972-883-4247.

ORCID

Shalini Prasad: 0000-0002-2404-3801

Author Contributions

H.S. and S.P. wrote the manuscript, S.S.S. and N.T. conducted electrochemical and FTIR experiments, H.S., S.S.S., and N.T. analyzed and interpreted the data.

Notes

The authors declare no competing financial interest.

REFERENCES

(1) Marshall, B. M.; Levy, S. B. Food animals and antimicrobials: impacts on human health. *Clin. Microbiol. Rev.* **2011**, *24*, 718–733.

(2) Holmes, A.; Holmes, M.; Gottlieb, T.; Price, L. B.; Sundsfjord, A. End non-essential use of antimicrobials in livestock. *Br. Med. J.* **2018**, *360*, k259.

(3) You, Y.; Silbergeld, E. K. Learning from agriculture: understanding low-dose antimicrobials as drivers of resistome expansion. *Front. Microbiol.* **2014**, *5*, 284.

(4) Van Boeckel, T. P.; Brower, C.; Gilbert, M.; Grenfell, B.; Levin, S. A.; Robinson, T.; Teillant, A.; Laxminarayan, R. Global trends in

DOI: 10.1021/acsomega.8b03534
ACS Omega 2019, 4, 6324–6330

antimicrobial use in food animals. *Proc. Natl. Acad. Sci. U.S.A.* **2015**, *112*, 5649−5654.
(5) Hughes, P.; Heritage, J. Antibiotic growth-promoters in food animals. *FAO Anim. Prod. Health Pap.* **2004**, 129−152.
(6) Tilman, D.; Balzer, C.; Hill, J.; Befort, B. L. Global food demand and the sustainable intensification of agriculture. *Proc. Natl. Acad. Sci. U.S.A.* **2011**, *108*, 20260−20264.
(7) Silva, N. C. C.; Guimarães, F. F.; Manzi, M. P.; Budri, P. E.; Gómez-Sanz, E.; Benito, D.; Langoni, H.; Rall, V. L. M.; Torres, C. Molecular characterization and clonal diversity of methicillin-susceptible Staphylococcus aureus in milk of cows with mastitis in Brazil. *J. Dairy Sci.* **2013**, *96*, 6856−6862.
(8) Zhu, Y.-G.; Johnson, T. A.; Su, J.-Q.; Qiao, M.; Guo, G.-X.; Stedfeld, R. D.; Hashsham, S. A.; Tiedje, J. M. Diverse and abundant antibiotic resistance genes in Chinese swine farms. *Proc. Natl. Acad. Sci. U.S.A.* **2013**, *110*, 3435−3440.
(9) Osterberg, D.; Wallinga, D. Addressing externalities from swine production to reduce public health and environmental impacts. *Am. J. Public Health* **2004**, *94*, 1703−1708.
(10) Massé, D.; Saady, N.; Gilbert, Y. Potential of biological processes to eliminate antibiotics in livestock manure: an overview. *Animals* **2014**, *4*, 146−163.
(11) Gassner, B.; Wuethrich, A. Pharmacokinetic and toxicological aspects of the medication of beef-type calves with an oral formulation of chloramphenicol palmitate. *J. Vet. Pharmacol. Ther.* **1994**, *17*, 279−283.
(12) White, D. G.; Zhao, S.; Sudler, R.; Ayers, S.; Friedman, B. A.; Chen, S.; McDermott, P. F.; McDermott, S.; Wagner, D. D.; Meng, J. The isolation of antibiotic-resistant Salmonella from retail ground meats. *N. Engl. J. Med.* **2001**, *345*, 1147−1154.
(13) Hiramatsu, K.; Katayama, Y.; Matsuo, M.; Sasaki, T.; Morimoto, Y.; Sekiguchi, A.; Baba, T. Multi-drug-resistant Staphylococcus aureus and future chemotherapy. *J. Infect. Chemother.* **2014**, *20*, 593−601.
(14) Organization, W. H. *The Medical impact of the use of antimicrobials in food animals: report of a WHO meeting*, Berlin, Germany, 1997, pp 13−17.
(15) Maron, D.; Smith, T. J.; Nachman, K. E. Restrictions on antimicrobial use in food animal production: an international regulatory and economic survey. *Global. Health* **2013**, *9*, 48.
(16) Fey, P. D.; Safranek, T. J.; Rupp, M. E.; Dunne, E. F.; Ribot, E.; Iwen, P. C.; Bradford, P. A.; Angulo, F. J.; Hinrichs, S. H. Ceftriaxone-resistant Salmonella infection acquired by a child from cattle. *N. Engl. J. Med.* **2000**, *342*, 1242−1249.
(17) Hornish, R.; Katarski, S. Cephalosporins in Veterinary Medicine—Ceftiofur Use in Food Animals. *Curr. Top. Med. Chem.* **2002**, *2*, 717−731.
(18) Dunne, E. F.; Fey, P. D.; Kludt, P.; Reporter, R.; Mostashari, F.; Shillam, P.; Wicklund, J.; Miller, C.; Holland, B.; Stamey, K.; Barret, T. J.; Rasheed, J. K.; Tenover, F. C.; Ribot, E. M.; Angulo, F. J. Emergence of domestically acquired ceftriaxone-resistant Salmonella infections associated with AmpC β-lactamase. *JAMA* **2000**, *284*, 3151−3156.
(19) Winokur, P. L.; Brueggeman, A.; DeSalvo, D. L.; Hoffman, L.; Apley, M. D.; Uhlenhopp, E. K.; Pfaller, M. A.; Doern, G. V. Animal and human multidrug-resistant, cephalosporin-resistant Salmonella isolates expressing a plasmid-mediated CMY-2 AmpC β-lactamase. *Antimicrob. Agents Chemother.* **2000**, *44*, 2777−2783.
(20) Schneider, M. J.; Lehotay, S. J. A comparison of the FAST, Premi and KIS tests for screening antibiotic residues in beef kidney juice and serum. *Anal. Bioanal. Chem.* **2008**, *390*, 1775−1779.
(21) Virolainen, N.; Karp, M. *Bioluminescence: Fundamentals and Applications in Biotechnology*; Springer, 2014; Vol. 2, pp 153−185.
(22) Lan, L.; Yao, Y.; Ping, J.; Ying, Y. Recent advances in nanomaterial-based biosensors for antibiotics detection. *Biosens. Bioelectron.* **2017**, *91*, 504−514.
(23) Lisdat, F.; Schäfer, D. The use of electrochemical impedance spectroscopy for biosensing. *Anal. Bioanal. Chem.* **2008**, *391*, 1555.
(24) Wang, J. Electrochemical biosensors: towards point-of-care cancer diagnostics. *Biosens. Bioelectron.* **2006**, *21*, 1887−1892.
(25) Vericat, C.; Vela, M. E.; Benitez, G.; Carro, P.; Salvarezza, R. C. Self-assembled monolayers of thiols and dithiols on gold: new challenges for a well-known system. *Chem. Soc. Rev.* **2010**, *39*, 1805−1834.
(26) Rudzinski, W. E.; Francis, K. Evaluating the surface density and heterogeneity of a dithiobis (succinimidylpropionate) self-assembled monolayer on gold and its coupling with DNA embedded within a matrix. *Appl. Surf. Sci.* **2010**, *256*, 5399−5405.
(27) Stevenson, H.; Shanmugam, N. R.; Selvam, A. P.; Prasad, S. The Anatomy of a Nonfaradaic Electrochemical Biosensor. *SLAS Technol.* **2018**, *23*, 5−15.

DOI: 10.1021/acsomega.8b03534
ACS Omega 2019, 4, 6324−6330